

Hybrid Compound SA-2 is Neuroprotective in Animal Models of Retinal Ganglion Cell Death

Dorota L. Stankowska,^{1,2} Adnan Dibas,^{1,2} Linya Li,³ Wei Zhang,^{1,2} Vignesh R. Krishnamoorthy,^{1,2} Sai H. Chavala,^{1,2} Tam Phung Nguyen,⁴ Thomas Yorio,^{1,2} Dorette Z. Ellis,^{2,3} and Suchismita Acharya^{1,2}

¹Department of Pharmacology and Neuroscience, University of North Texas Health Science Center, Fort Worth, Texas, United States

²North Texas Eye Research Institute, University of North Texas Health Science Center, Fort Worth, Texas, United States

³Department of Pharmaceutical Sciences, University of North Texas Health Science Center, Fort Worth, Texas, United States

⁴Department of Bioengineering, The University of Texas at Arlington, Arlington, Texas, United States

Correspondence: Suchismita Acharya, Department of Pharmacology and Neuroscience, North Texas Eye Research Institute, University of North Texas Health Science Center, 3500 Camp Bowie Boulevard, Fort Worth, TX 76107, USA; suchismita.acharya@unthsc.edu.

Submitted: October 16, 2018

Accepted: June 8, 2019

Citation: Stankowska DL, Dibas A, Li L, et al. Hybrid compound SA-2 is neuroprotective in animal models of retinal ganglion cell death. *Invest Ophthalmol Vis Sci.* 2019;60:3064-3073. <https://doi.org/10.1167/iov.18-25999>

PURPOSE. Determine the toxicity, bioavailability in the retina, and neuroprotective effects of a hybrid antioxidant-nitric oxide donor compound SA-2 against oxidative stress-induced retinal ganglion cell (RGC) death in neurodegenerative animal models.

METHODS. Optic nerve crush (ONC) and ischemia reperfusion (I/R) injury models were used in 12-week-old C57BL/6J mice to mimic conditions of glaucomatous neurodegeneration. Mice were treated intravitreally with either vehicle or SA-2. Retinal thickness was measured by spectral-domain optical coherence tomography (SD-OCT). The electroretinogram and pattern ERG (PERG) were used to assess retinal function. RGC survival was determined by counting RBPMS-positive RGCs and immunohistochemical analysis of superoxide dismutase 1 (SOD1) levels was carried out in the retina sections. Concentrations of SA-2 in the retina and choroid were determined using HPLC and MS. In addition, the direct effect of SA-2 treatment on RGC survival was assessed in ex vivo rat retinal explants under hypoxic (0.5% O₂) conditions.

RESULTS. Compound SA-2 did not induce any appreciable change in retinal thickness, or in a- or b-wave amplitude in naive animals. SA-2 was found to be bioavailable in both the retina and choroid after a single intravitreal injection (2% wt/vol). An increase in SOD1 levels in the retina of mice subjected to ONC and SA-2 treatment, suggests an enhancement in antioxidant activity. SA-2 provided significant ($P < 0.05$) RGC protection in all three of the tested RGC injury models in rodents. PERG amplitudes were significantly higher in both I/R and ONC mouse eyes following SA-2 treatment ($P \leq 0.001$) in comparison with the vehicle and control groups.

CONCLUSIONS. Compound SA-2 was effective in preventing RGC death and loss of function in three different rodent models of acute RGC injury: ONC, I/R, and hypoxia.

Keywords: neuroprotection, SOD, nitric oxide, hybrid small molecule, RGC, glaucoma

Retinal ganglion cells (RGCs) are output neurons that ultimately transmit visual information from the retina to the brain. Irreversible blindness worldwide¹ due to RGC degeneration includes ischemic optic neuropathies, hereditary optic neuropathies, and glaucoma. RGCs are highly susceptible to oxidative stress and ischemic insult.^{2,3} Primary open angle glaucoma and angle-closure glaucoma are characterized by elevated IOP, axonal degeneration of the optic nerve, and progressive loss of RGCs. The current approaches to slow down glaucomatous vision loss are mainly aimed at lowering IOP, which do not fully address the susceptibility to RGC degeneration.⁴

Artery, vein occlusion, or elevated IOP produce oxidative stress in both RGCs and retinal endothelial cells through decreased activity of several antioxidant enzymes, including superoxide dismutase (SOD), glutathione peroxidase, catalase, and thioredoxins (Trx1 and Trx2), and these imbalances have been implicated in promoting RGC death.⁵⁻⁷ Ischemic stress in the eye followed by reperfusion generates an outburst of detrimental superoxide free radicals. The superoxide radicals then induce oxidative stress, leading to apoptosis of RGCs⁸ as

well as dysfunction of retinal endothelial cells. Another factor contributing to ischemic neuronal damage is N-methyl-D-aspartate (NMDA)-induced entry of calcium followed by production of free radicals.⁹ In the rat hippocampus,¹⁰ the activation of NMDA receptors generates reactive oxygen species (ROS) and decreases antioxidant potential of the tissue. Furthermore, the toxic peroxynitrite¹¹ formed from the reaction of NO and superoxide anions (O₂⁻) is responsible in part for NMDA receptor-mediated neurotoxicity. Cellular SOD enzymes convert the O₂⁻ radical to O₂ and H₂O₂. In many chronic and acute neurodegenerative diseases, including glaucomatous optic neuropathy,^{12,13} decrease in SOD has been associated with oxidative stress-induced neurotoxicity. SOD is an enzyme that includes three forms: SOD1 (Cu, Zn-SOD), SOD2 (Mn-SOD), and SOD3 (containing Zn and Cu) encoded by separate genes.¹⁴ Deficiency in SOD1 but not SOD2 is known to cause RGC sensitivity to various insults, which may be the underlying condition of normal tension glaucoma.¹⁵ Significantly higher levels of superoxide anions were found in the RGC layer of 24-week-old SOD1-deficient mice compared with



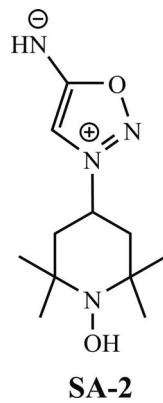


FIGURE 1. Chemical structure of compound SA-2.

wild-type mice.¹⁵ Such an elevation of ROS can lead to RGC death if they persist.

Several studies have also demonstrated that nitric oxide (NO) has neuroprotective properties mediated through the induction of the cyclic guanosine monophosphate (cGMP) pathway in hippocampal neural cells.^{16–18} This occurs primarily by the ability of cGMP to promote vasodilation and consecutively increase blood supply to neurons, reduce oxidative stress, and minimize Ca^{2+} influx through inhibition of NMDA receptors at the glutamatergic synapses of neurons. Multiple evidence has documented that, besides NO bioavailability, its concentration in the tissue is crucial for its action. At nanomolar to low micromolar concentrations, NO exhibits diverse effects, including protection against endothelial dysfunction, vasodilatation of smooth muscle cells (SMCs), and proliferation of endothelial cells.^{19,20} However, high concentrations of NO (millimolar) lead to detrimental effects, including formation of peroxynitrite radical, nitrosylation of proteins, which could ultimately result in apoptosis. Therefore, it is essential to balance the level of NO bioavailability and amount of superoxide in the retina to preserve the cellular homeostasis.

Recently, we reported²¹ a novel hybrid molecule SA-2 (Fig. 1) that combines a SOD mimetic to scavenge the superoxides, and an NO donor to maintain NO bioavailability. This unique combination protects RGCs from death and has the potential to be an efficacious neuroprotective treatment for glaucoma. This current study examines the neuroprotective effects of SA-2 demonstrated in three models of RGC injury; ex vivo rat retinal explant hypoxia model, and two in vivo mouse models: optic nerve crush (ONC) and ischemia/reperfusion (I/R).

Our results from three rodent models demonstrated that both prophylactic and therapeutic intravitreal dosing of the hybrid compound SA-2 are protective in the retina and RGCs. Moreover, compound SA-2 does not exhibit toxicity in the retina and is bioavailable in both the retina and the choroid after a single intravitreal injection. The immunohistochemistry demonstrated an increase in SOD1 intensity in the SA-2-injected retinas, including ganglion cell layer (GCL), demonstrating improvement in antioxidant activity by SA-2.

METHODS

Animals

All animal studies were performed in accordance with the ARVO Statement for the Use of Animals in Ophthalmic and Vision Research and approved by the University of North Texas Health Science Center Institutional Animal Care and Use

Committee. For the ONC and ischemia reperfusion studies, we used 5- to 6-month-old C57BL/6J mice from Charles River (Wilmington, MA, USA). Adult female Sprague-Dawley rats (8 to 10 weeks old) were obtained from Charles River and used for ex vivo studies.

Intravitreal Injections of Test Compound

Compound SA-2 was prepared as a hydrochloride salt in our laboratory following the synthetic procedure as reported earlier.²¹ ATN-224 was purchased from Cayman Chemicals (Ann Arbor, MI, USA; CAS No. 649749-10-0). For intravitreal injections, SA-2 was dissolved in prefiltered, sterile buffered balanced salt solutions (pH 7.5). Intravitreal injections using a Hamilton syringe with a 32-gauge needle were done using a dissecting microscope. The mice were anesthetized by intraperitoneal injection of ketamine (95 mg/mL, Ketaved) and xylazine (5 mg/mL; Sigma Aldrich, St. Louis, MO, USA) (100 μ L/100 g). A drop of 0.5% proparacaine hydrochloride and 1% tropicamide (Alcon Laboratories, Inc., Fort Worth, TX, USA) was applied to both eyes. Intravitreal injections (2 μ L per eye) were performed through the sclera, approximately 1 mm behind the limbus where the solution was slowly (approximately 30 seconds) injected into the vitreous chamber of the eye. After injection, the needle was held in the eye for at least 30 seconds to prevent leakage and facilitate mixing before withdrawing the needle. Two microliters of 2% (75 mM) SA-2 provided 75 picomolar concentration of SA-2 in the retina after a single injection. Hence, we used either 1% or 2% of SA-2 for all the in vivo experiments.

Optical Coherence Tomography (OCT)

OCT was done using Reveal OCT2 Imaging System (Phoenix Research Laboratories, Pleasanton, CA, USA) with a contact lens specifically designed for mice. Mice were anesthetized by an inhalation of isoflurane. Eyedrops of 0.1% Tropicamide (Akorn, Inc., Lake Forest, IL, USA) was used to dilate the pupils. A drop of GenTeal liquid gel (Novartis, East Hanover, NJ, USA) was applied to the cornea to prevent drying. The mice ocular fundus was monitored with the fundus camera of the Micron IV imaging system (Phoenix Research Laboratories). Three positions of the retinal OCT images from the same eye were set horizontally across the optic disc, one-disc diameter superior and one inferior to the optic disc. Ten to 20 images at the same positions were averaged to eliminate artifacts.

Electroretinogram

Before ERG measurements, the animals were dark adapted and kept under dim red light. After 12 hours of dark adaptation, mice were anesthetized by inhalation of isoflurane. Pupils were dilated using 0.1% Tropicamide eye drops and the corneal surface was kept moist with GenTeal liquid gel. During the measurements, the animals were kept on a heating pad. One needle probe was inserted subcutaneously for reference between the two eyes. A silver needle placed in the proximal part of the tail served as the ground electrode. The contact lens electrode (Micron IV Ganzfield ERG; Phoenix Research Laboratories) was placed directly over the cornea. For the measurements of scotopic response, light stimulus intensities were set as $-1, 0, 1, 1.5 \text{ Log (cd.s/m}^2\text{)}$. Five sweeps were recorded at each light intensity with sufficient delay between each sweep. The average of five responses to the same stimulus intensity was used as the final waveform for the certain light stimulus. The amplitudes of both a-waves and b-waves were analyzed.

SA-2 Biodistribution

The ocular concentration of compound SA-2 was measured using the retinal, choroidal, and scleral tissues using a published protocol in mouse eyes.²² This experimental approach was chosen because the retina and choroid are typically the targets of neuroprotective treatments. The injected eyes were enucleated 1 hour following intravitreal (ivt) injection to measure concentration of the drug in the retina. Twelve eyes were analyzed. Each individual sample contained four whole retinas or four choroids plus scleral tissues extracted from four eyes. Initially, 100 μ L of cold PBS was added to the samples and homogenized for 6 min with motorized pestle (#47747-370; VWR International LLC, Radnor, PA, USA). Subsequently, 900 μ L of acetonitrile at 4°C was added and mixture was vigorously mixed for 2 minutes and then ultracentrifuged at 68,000g for 20 minutes at 4°C. The supernatant was concentrated using a Vacufuge Plus (Eppendorf, New Brunswick, Germany) and reconstituted with a mixture of 40 μ L of 10:1 water:acetonitrile. The SA-2 standard was dissolved in 50% acetonitrile containing 0.05% (vol/vol) formic acid and vortexed for 60 seconds. All samples and standards were filtered through a 0.45- μ m Acrodisc (Manufacturer, City, State, Country) 3 CR PTFE filter to be devoid of insoluble particles prior to injecting into a C18 HPLC column (Luna Polar C18 100x1 1.6 μ m; Phenomenex, Torrance, CA, USA). The samples were analyzed using Shimadzu (Kyoto, Japan) gradient HPLC (Shimadzu LCMS-8050) in a system of 0.05% formic acid in water (buffer A) versus 0.05% formic acid in acetonitrile (buffer B) at a flow rate of 0.07 mL/min. A 20- μ L volume of each sample was injected into the Luna Polar C18 100x1 1.6 μ m, Phenomenex, which was pre-equilibrated with 50% buffer B. Compound SA-2 was eluted with 50% acetonitrile containing 0.05% formic acid for 15 minutes. SA-2 peak was visualized at 254 nm using a Shimadzu LC-30AD UHPLC. The standard curve composed of nine different concentrations of SA-2 standard was linear in ranges between 0.06 and 15.6 pg/mL (correlation coefficient $r^2 = 0.9991$). The detection limit was estimated to be nearly 9.0 pmol (signal-to-noise ratio greater than 2). The below equation was used for the one-compartment model:

$$C(t) = \frac{\text{Dose}}{V_d} \times \exp^{-kt},$$

where $C(t)$ represents the quantity of SA-2 at time t , V_d signifies the volume of distribution. The data were also analyzed using a noncompartmental model for reference.

Ex Vivo Rat Retinal Explants Model

The rat organotypic retinal explant cultures were prepared as published by us previously.²³ Four to five explants isolated from each retina were incubated with the RGC layer facing up on Transwell Permeable 6.5-mm inserts. A control group of retinal explants were maintained in 5% CO₂ at 35°C or at 37°C (normoxia) in an explant medium composed of phenol red free Neurobasal A supplemented with 2% B27 1% N₂, 0.8 mM L-glutamine, 100 U/mL penicillin, and 100 μ g/mL streptomycin (all reagents from Thermo Fisher Scientific, Waltham, MA, USA). One group of retinal explants following 1 hour of equilibration at normoxic conditions was moved to a hypoxic chamber in which the injection of nitrogen gas produced steady state of 0.5% O₂. Some retinal explants were treated with either SA-2 (1 μ M) or dimethyl sulfoxide (DMSO) (0.01%, vehicle) for 18 hours at normoxic or hypoxic conditions. Following the treatments, the explants were fixed with 4% paraformaldehyde at 4°C for 24 hours, blocked with blocking buffer (5% normal donkey serum, 5% BSA in PBS), and incubated with the primary antibody: goat anti-Brn3b (dilution

1:500; Santa Cruz, Dallas, TX, USA) antibody at 4°C for 72 hours. Subsequently, fluorescently labeled secondary antibody (donkey anti-goat Alexa 647; Invitrogen, Carlsbad, CA, USA) was added, incubated for 24 hours at 4°C, and retinal explants were mounted with ProlongDiamond (Invitrogen) on glass slides. The retinal explants from two independent experiments ($n = 4$ explants per group from four Sprague-Dawley rats) were imaged using Zeiss (Oberkochen, Germany) LSM 510 Meta scanning confocal microscope. The number of surviving, Brn3a-positive cells in each explant was manually counted by an masked observer with cell counter plugin (<http://imagej.nih.gov/ij/>; provided in the public domain by the National Institutes of Health, Bethesda, MD, USA) as previously reported²³ and statistical analysis was performed using 1-way ANOVA followed by the Student-Newman-Keuls post hoc test, using the SigmaPlot software (Systat Software, Inc., San Jose, CA, USA) with $P < 0.05$ considered to be statistically significant.

Mouse Model of ONC

The ONC model was performed using C57BL/6J mice in one eye and the contralateral eye served as control. Mice were anesthetized by intraperitoneal injection of ketamine (100 mg/kg) and xylazine (10 mg/kg) and ONC was performed as previously described.²⁴ Briefly, one optic nerve was exposed intraorbitally through a small incision made between the surrounding muscles following which the optic nerve, approximately 1 mm behind the globe, was crushed with self-closing forceps for 4 seconds under visualization in a microscope. At the endpoints of the experiments, animals were euthanized, eyes were enucleated, and RGCs were quantified as described below. Compound SA-2 (either 1% or 2% solution in PBS) was intravitreally injected in mice at days 0 and 3 following ONC surgery. We reported earlier that²¹ compound SA-2 possesses a short half-life ($t_{1/2} < 1$ day); therefore, we injected two doses 3 days apart anticipating to achieve therapeutic level of SA-2 in retina. The 0-day and 3-day dosing regimen was selected to provide sufficient time between the two doses and allow healing of the ivt injection-related injury of the mouse eye from the first dose.

Ischemic-Reperfusion (I/R) Retina Injury With an Acute IOP Elevation

Compound SA-2 (2%) was injected intravitreally 48 hours before the I/R surgery. I/R was performed in one eye as previously described by Dibas et al.²⁴ Briefly, anesthetized C57BL/6J mice were placed on a heating blanket to prevent hypothermia. The 0.5% proparacaine (Bausch & Lomb Pharmaceuticals, Tampa, FL, USA) was applied to the corneas and the pupils were dilated using minims phenylephrine hydrochloride 2.5% wt/vol (Bausch & Lomb Pharmaceuticals). A 32-gauge needle was injected into the anterior chamber through the cornea. The PBS reservoir attached to the needle was elevated to increase IOP to 120 mm Hg. Ischemia was confirmed by an observation of blanching of the anterior segment and arteries in the eye. Contralateral eyes were used as untreated controls. Following 60 minutes of ischemia, the needle was removed to allow rapid reperfusion. Sham procedures were performed in a separate cohort of mice whereby a needle was inserted into the anterior chamber, and pressure in the eye was not increased (PBS reservoir was not elevated), hence ischemia was not produced. Previously published experiments using a sham control demonstrated no difference from contralateral controls.

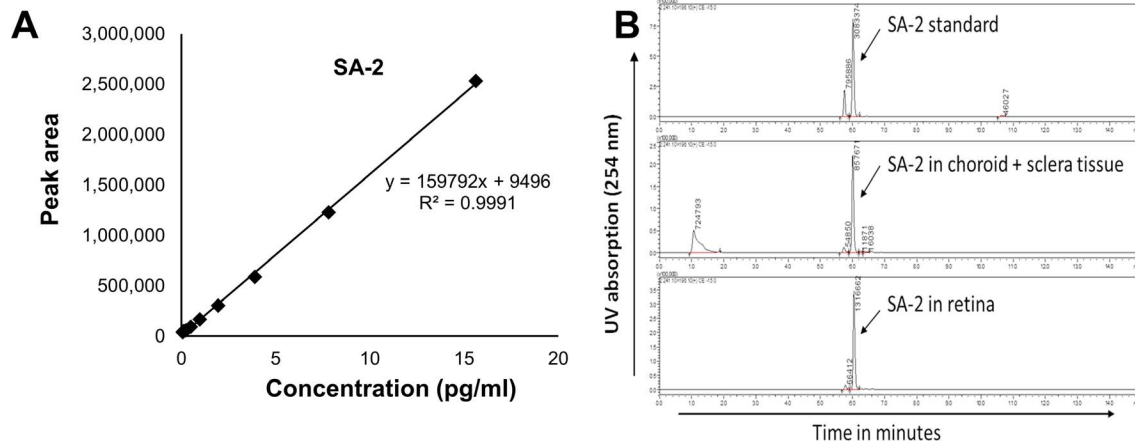


FIGURE 2. Bioavailability of SA-2 (2% wt/vol) in the retina and choroid tissues after single ivt dosing in mice. **(A)** Standard curve for detecting SA-2 using HPLC. **(B)** HPLC chromatogram showing the detection of compound SA-2 in tissues choroid/sclera tissues, $n = 12$ eyes.

RGC Counts Following ONC

RGCs were quantified in fixed retinal flat mounts by immunostaining with the anti-RNA Binding Protein with Multiple Splicing (RBPMs) antibody (GTX118619, dilution 1:200; GeneTex, Irvine, CA, USA) as published previously²³ with modifications. Eight images were taken from peripheral and mid-peripheral regions around four quadrants of each retina. The number of cells in a total of four equal-sized fields (0.02 mm² retina area) were counted and averaged as previously reported.²⁵ The data were presented as mean \pm SEM and the cell count was performed in a masked manner.

Pattern ERG

PERG was used to measure the function of RGCs by recording the amplitude of the PERG waveform following ONC or I/R injury in mice, as previously described.²⁶ Animals were anesthetized and placed on a heated stage and PERG responses were evoked in response to contrast reversal of patterned visual stimuli using commercially available PERG system (Jorvec, Inc., Miami, FL, USA). The PERG responses were acquired in the red-light environment from a needle electrode placed sub-dermally in the mice snout, the reference was placed on the base of the head, and the ground electrode was placed at the base of the tail. Each animal was positioned at 11 cm from the display monitors. Stimuli (45° radius visual angle subtended on full-field pattern, two reversals per second, 300 averaged signals with cutoff filter frequencies of 1–30 Hz, 98% contrast, 800 cd/m² average monitor illumination intensity) were delivered without dark adaptation to exclude the possible effect of direct photoreceptor-derived evoked responses. The PERG amplitudes at baseline and 7 days following ONC or I/R injury were calculated as previously described.²⁵

Immunohistochemistry

Five-micrometer-thick mouse sagittal retinal sections through the optic nerve head were obtained from mice eyes from the 7 days post ONC + PBS ($n = 3$) and ONC + SA-2 ($n = 5$) treatment groups. Then sections were deparaffinized in xylene (Thermo Fisher Scientific, Fairlawn, NJ, USA), and rehydrated using a series of ethanol washes (100%, 95%, 90%, 80%, and 50%). Blocking was performed using 5% normal donkey serum and 5% BSA in PBS to prevent nonspecific binding of the secondary antibody. Following blocking, the sections were incubated with primary antibodies: mouse anti- β III Tubulin antibody

(Sigma Aldrich, and diluted 1:1000), rabbit polyclonal to Superoxide Dismutase 1-SOD1 antibody (ab13498, diluted 1:1000) or mouse monoclonal anti-3-Nitrotyrosine antibody (ab110282, 1 μ g/mL)²⁷ and incubated for 24 hours at 4°C. Secondary antibody incubation was carried out for 1 hour with a 1:1000 dilution of the appropriate secondary antibodies. Sections in which the primary antibody incubation was omitted were used to assess nonspecific staining by the secondary antibodies. DAPI (4',6-diamidino-2-phenylindole) was used to visualize nuclei. Fluorescence images were captured using a Zeiss LSM 510 META confocal microscope ($\times 40$) or Cytation5 (BioTek Instruments, Winooski, VT, USA) at $\times 20$ magnification. Retinal sections, were imaged as detailed above and analyzed by a masked observer to treatment groups. β III Tubulin-positive and DAPI-positive cells were counted in radial sections of the retina, along a linear region of the RGC layer on both sides of the optic nerve head. The SOD1 fluorescence intensity was calculated using ImageJ software from the whole retinas, whereas β III Tubulin and DAPI-positive cells in the GCL were manually counted by a masked observer and all were presented as mean \pm SEM.

RESULTS

SA-2 Is Localized in Retina and Choroid Following Single Intravitreal Dosing

The peak SA-2 concentration was calculated according to appropriate standard curves using the LC solution software. These standard curves, created using nine different concentrations of SA-2, were linear from 0 to 15.6 pg/mL (correlation coefficient >0.9991). The detection limit was below 0.06 pg/mL and is within the linear limits of detection. Compound SA-2 was detectable in both retina and choroid + sclera samples collected 1 hour following the injection into six mice ($n = 12$ eyes) as shown in Figure 2. The maximum concentration of SA-2 was found to be 75 pmol and 230 pmol in retina and choroid plus sclera tissues, respectively, from a single ivt injection of 2 μ L of SA-2 (2%).

SA-2 Is Not Toxic to Retina

Spectral-domain OCT (SD-OCT) was performed day 0 and 7 days following injection of 2% of compound SA-2 in mouse eyes ($n = 2-6$). Changes in the amplitudes of the scotopic a-wave and b-wave in response to an increasing stimulus

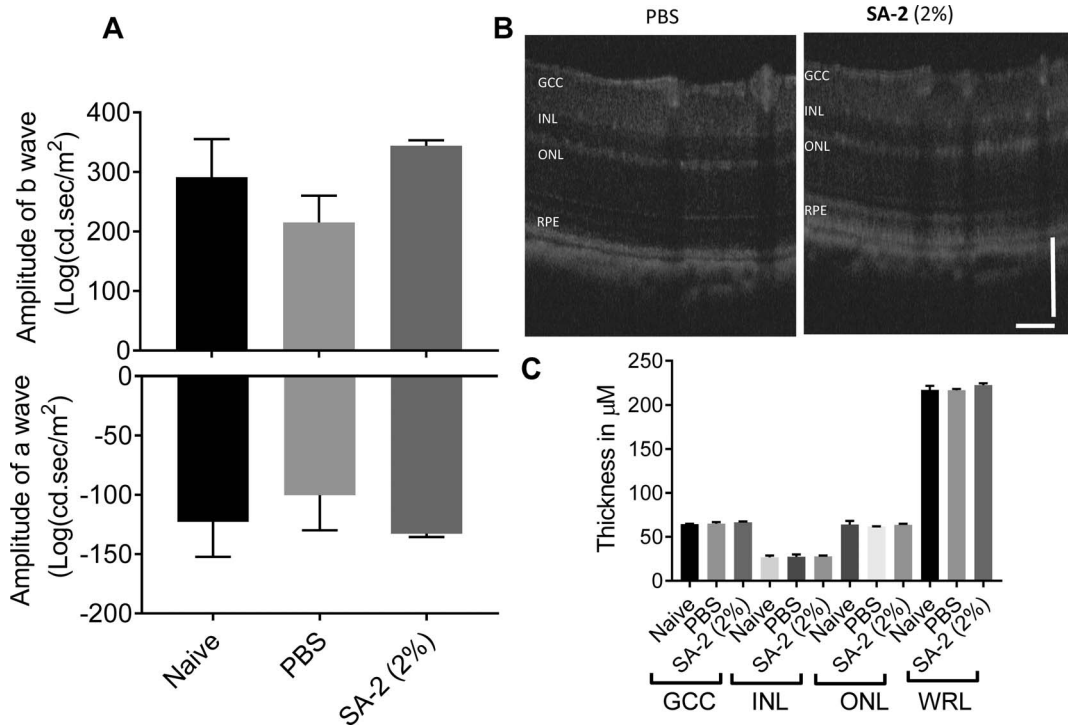


FIGURE 3. Single ivt injection of SA-2 (2% wt/vol) to C57BL/6J mouse eyes did not cause any toxicity to the retina. **(A)** Compound SA-2 did not induce scotopic ERG changes. The a- and b-wave amplitudes of scotopic ERG at 1 Log (cd.sec/m²) light intensity were measured in the vehicle and SA-2-treated eyes 7 days after treatment. Data represent mean \pm SD ($n = 2-6$ eyes). Two-way ANOVAs indicated no significant changes between the PBS group and SA-2-treated groups. **(B)** Representative images are shown, and the graph illustrates the mean thickness of analyzed layers. Ten days after treatment with 2% SA-2, there were no thickness changes. **(C)** SD-OCT was used to determine the changes in whole retinal layer (WRL; from NFL to RPE), and each of GCC, INL, and ONL. Two-way ANOVA indicated that there were no significant differences between the vehicle (PBS) and SA-2 groups at each layer ($n = 2$ mice per group). GCC, ganglion cell complex including NFL, GCL, and IPL; INL, inner nuclear layer; NFL, nerve fiber layer; ONL, outer nuclear layer; RPE, retinal pigment epithelium.

intensity was measured. The results clearly demonstrated no significant differences in ERG response of a-waves (-122.8 ± 26.82 Log cd.sec/m²) for naïve and (-132.75 ± 2.05 Log cd.sec/m²) for SA-2 treated eyes and b-waves (291.21 ± 58.45 Log cd.sec/m²) for naïve and (344.1 ± 8.9 Log cd.sec/m²) for SA-2 treated eyes (Fig. 3A). In addition, there were no significant changes in the overall thickness of the retina (Fig. 3B, 3C) suggesting no retinal toxicity at this dose.

Compound SA-2 Is Neuroprotective Against Hypoxia-Induced RGC Death in Rat Ex Vivo Organotypic Retinal Explant Model

To demonstrate the direct neuroprotective potential of compound SA-2 on RGCs, we used an ex vivo model of retinal explants isolated from adult Sprague-Dawley rats. The explants were incubated at normoxic and hypoxic (oxygen deprivation) conditions either in the presence or absence of SA-2 (1 μ M) for 18 hours, and the number of surviving Brn3a-positive RGCs was measured (Fig. 4A, 4B). The dose (approximately $2.5 \times$ half maximal effective concentration [EC₅₀]) for this experiment was selected based on our previous report²⁸ whereby compound SA-2 protected human umbilical vascular endothelial cells (HUVECs) from H₂O₂-induced oxidative stress with EC₅₀ of 0.354 μ M, and demonstrated an increase in cell viability. SA-2 was not toxic to RGC in normoxic condition with RGC counts of $2307 \pm 228/\text{mm}^2$ in comparison with the 0.001% DMSO (vehicle)-treated group (2280 ± 315 RGCs/mm²). During hypoxia the compound SA-2 provided statisti-

cally significant (1673 ± 146 RGCs/mm², $P < 0.05$) protection of RGCs in comparison with the vehicle group (868 ± 74 RGCs/mm²). These data suggest that compound SA-2 significantly protected the RGCs against the hypoxic injury.

Compound SA-2 Prevents I/R Injury-Mediated RGC Loss and Improves RGC Function

We evaluated the effect of single ivt injection of SA-2 (2%) on RGC function following an I/R insult. We selected that dose based on the biodistribution study (Fig. 2) in which a single ivt injection of 2% SA-2 provided 75 to 230 pmol concentration of SA-2 in retina and choroid tissues. The PERG was analyzed 7 days²⁹ after I/R to determine whether single SA-2 intravitreal injections (48 hours before I/R) could prevent the decline in PERG amplitude usually observed at that time point following I/R procedure. Representative PERG waveforms recorded from the eyes in each group are shown in Figure 4C. PERG amplitudes of PBS-injected and I/R-injured, SA-2-injected and I/R-injured, as well as the sham-operated mouse retinas were compared (as shown in Fig. 4D). The average PERG amplitude of sham mice was 30.1 ± 2.5 μ V ($n = 8$), whereas the average PERG amplitude of PBS-treated-I/R mice was significantly reduced (5.1 ± 0.3 μ V, $n = 5$, $P < 0.05$ versus sham). However, the average PERG amplitude and I/R SA-2-pretreated mice were significantly higher when compared with I/R- and PBS-treated mice (11 ± 2.3 μ V, $P < 0.05$, $n = 5$) suggesting partial rescue of RGC function.

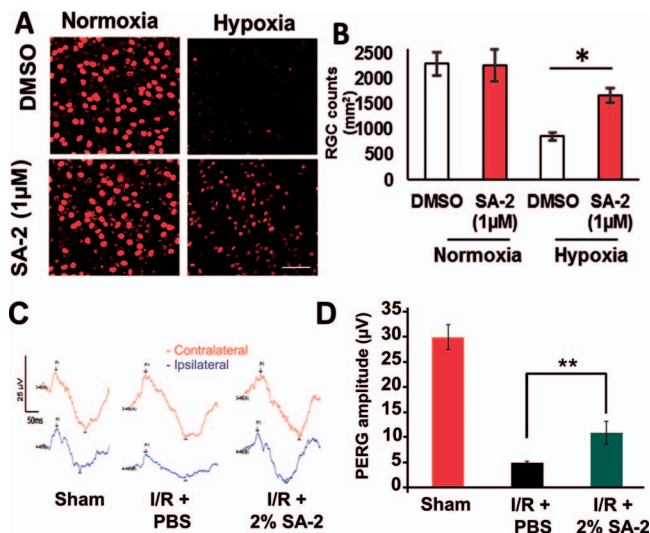


FIGURE 4. Compound SA-2 was neuroprotective to adult rat RGC explants under hypoxic condition and partially restored RGC function following 7 days post-I/R in C57BL/6J mice. (A) Retinal explants were treated with SA-2 (1 μM) or vehicle in a normoxic and hypoxic conditions. RGCs labeled with RGC marker Brn3a, in red, were counted to determine changes in their viability. The graph (B) shows quantification of RGC counts per mm² of the retinal explant. Vehicle (DMSO) treatment resulted in significantly lower RGC number than the SA-2 group exposed to hypoxia. **P* < 0.05. One-way ANOVA with Student-Newman-Keuls Method, *n* = 4 explants per group. (C) Sample PERG waveforms recorded from the ipsilateral and contralateral eyes following ivt injections of SA-2 (2%) and I/R injury to the pattern stimulus. (D) Analysis of PERG amplitudes in mice exposed to I/R and pretreated with 2% of SA-2 showed significant difference compared with PERG amplitudes from sham-injured control mice. Sham mice did not display any evidence of functional RGC deficits 7 days (30.1 ± 2.5 μV, *n* = 8) after mock surgery; however, there was a significant decrease in I/R-injured and PBS-treated mice compared with PERG amplitudes from sham mice (5.1 ± 0.3 μV, *n* = 5). Single ivt injection pretreatment with compound SA-2 (2%) statistically increased PERG amplitude compared with PBS-treated I/R mice (11 ± 2.3 μV, *n* = 5, ***P* < 0.05 using 1-way ANOVA).

Compound SA-2 Protects RGC From Cell Death and Preserves RGC Function Following Acute Axonal Injury (ONC) in Mice

To further assess the neuroprotective effects of SA-2, mice were subjected to ONC, an acute axonal injury model, and then treated with either PBS or two doses of SA-2 (ivt injection of 2 μL of either 1% or 2% wt/vol) at day 0 and day 3 following

the crush. Unoperated eyes served as contralateral controls for ONC. Figure 5B demonstrates confocal images of RBPMS-stained retinas from 7 days post ONC with 1% SA-2 treatment. There was a statistically significant higher number of RBPMS-positive RGCs in ONC + 1% SA-2-treated group (1454.03 ± 78.30/mm²) when compared with ONC + PBS cohort (960.429 ± 46.311/mm²), clearly demonstrating the neuroprotective ability of SA-2 after ONC in mice (Fig. 5A). Encouraged by this finding, we further investigated a higher dose SA-2 (2%) in ONC mouse model. RGC function was measured using PERG. The PERG amplitude was significantly greater and the latency was significantly lower in eyes from ONC + 2% SA-2-treated mice than in eyes from ONC + PBS-treated mice. Significant differences in PERG amplitudes were observed in mouse eyes (*n* = 6) with crushed optic nerve in comparison to contralateral controls (*P* ≤ 0.001). There was a dose-dependent restoration of PERG amplitudes observed at 1% (6.3 ± 0.699 μV) vs. 2% (7.93 ± 0.735 μV) doses of SA-2 treated eyes compared with PBS-treated ONC mice (5.04 ± 0.714 μV) eyes as shown in Figures 5C and 6B, respectively. To understand if the neuroprotective effect is truly due to upregulation of SOD or not, we performed an experiment with a known SOD1 inhibitor ATN-224 is a membrane-permeable copper chelator.^{30,31} Initially, we screened different doses of ATN-224 in mouse eyes (*n* = 6 eyes per dose) via ivt injection of ATN-224 (3.12, 6.25, 12.0, and 25.0 μg/mL). ERG analysis was performed 7 days after ONC surgery. We did not observe any change in b-wave at both 3.15-μg/mL and 6.12-μg/mL doses (Fig. 6A). Thus, 3.15 μg/mL was selected for the combination study. As expected, the protective effect of SA-2 was diminished by coadministration of 3.12 μg/mL of ATN-224 with 2% SA-2. The effect was measured by both RBPMS-stained RGC counts (Fig. 6D, 6E, 995 ± 50.8/mm² for ONC + 2% SA-2 eyes and 906.991 ± 43.45/mm² for SA-2 + ATN-224 eyes) and PERG (Fig. 6B, 7.93 ± 0.735 μV for ONC + 2% SA-2 eyes and 5.22 ± 0.75 μV for SA-2 + ATN-224 eyes). This confirmed the SOD-mediated neuroprotective effect of SA-2 in the retina.

To further evaluate the change in the levels of SOD1 enzyme in the retina, mouse retina sections were subjected to immunohistochemical analysis. As seen in Figure 6F, an increased SOD-1 immunostaining (in yellow) was detected in ONC + SA-2-treated retinas mainly in GCL, the inner plexiform layer (IPL), and outer plexiform layer (OPL) in comparison with ONC and PBS-treated group in which minimal SOD1 staining was observed. The SOD-1 staining in GCL was evident mainly in the cytoplasm of RGCs, similar to previously published reports.³² βIII tubulin was used as an RGC marker as previously published by us²³ and DAPI was used to detect the nuclei. There was an increased SOD1 fluorescence intensity (Fig. 6G) in the immunolabeled retinas of ONC + 2% SA-2 group

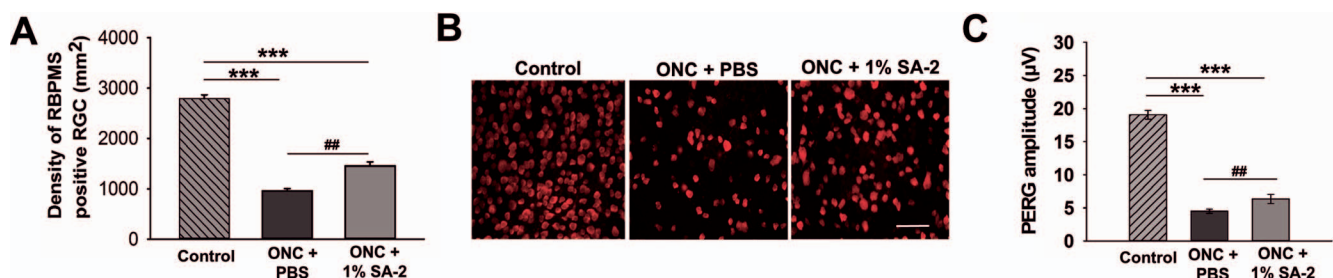


FIGURE 5. Effects of ivt injections of 1% SA-2 in C57BL/6J mice following ONC. (A) RBPMS-labeled RGCs were counted in mice retinas (*n* = 6 per group). A significant (**P* < 0.001) decline in RGC counts was observed 7 days following ONC in comparison with the contralateral controls. There was a statistically significant protection of RGCs (#*P* < 0.05) between ONC, ONC + SA-2 (1%)-treated cohort versus ONC + PBS-treated group. (B) Representative fluorescence images of RBPMS-labeled RGCs in contralateral and ONC mouse retinas. Scale bar: 50 μm. (C) PERG amplitudes observed at 1% dose of SA-2 (6.3 ± 0.699 μV, *n* = 5) dose of SA-2 compared with PBS-treated ONC mice (5.04 ± 0.714 μV, *n* = 5), ##*P* < 0.05 and ****P* < 0.001 using 1-way ANOVA, Student-Newman-Keuls Method. Values signify mean ± SEM.

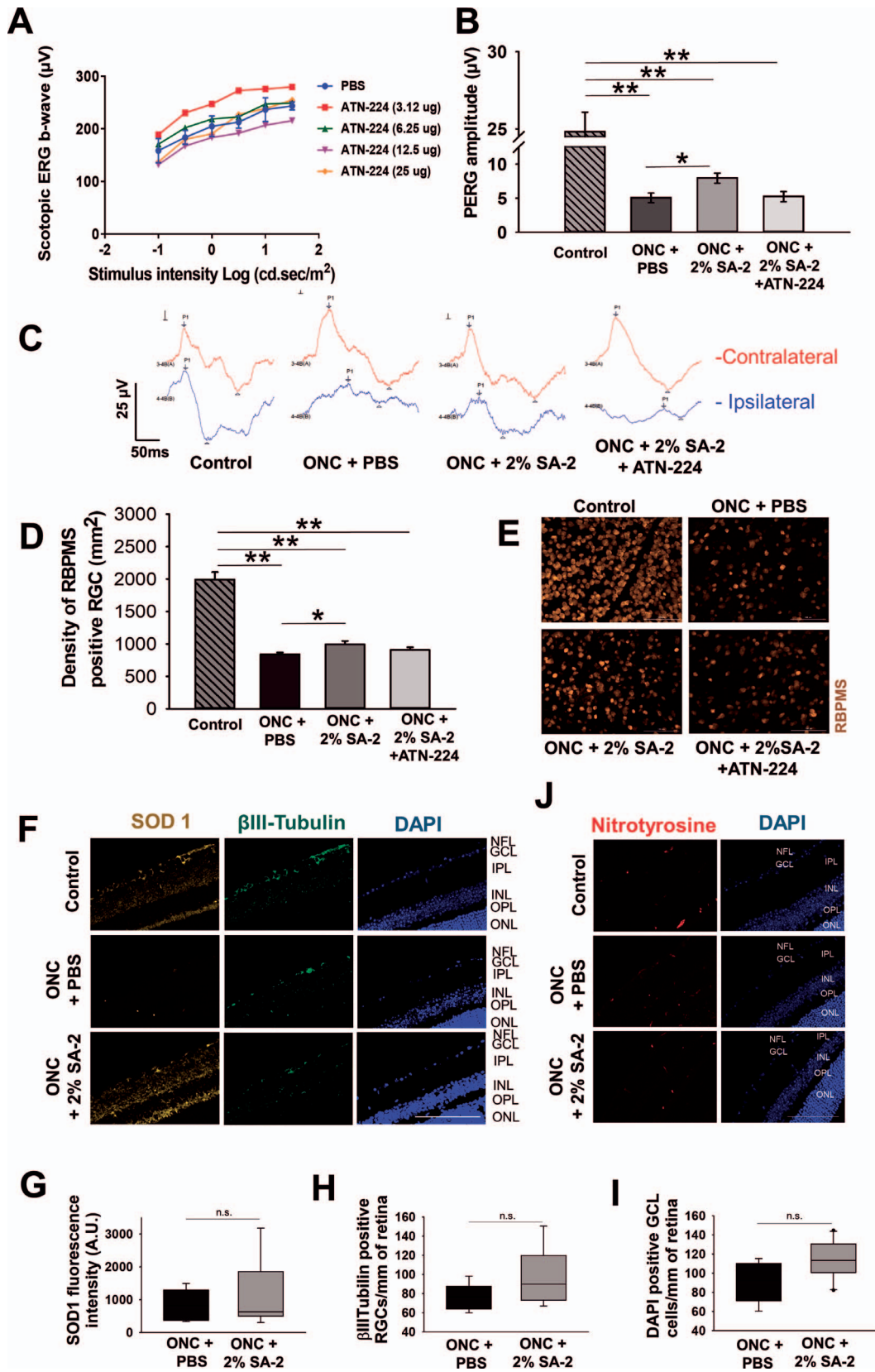


FIGURE 6. Effects of ivt injections of 2% SA-2 in C57BL/6j mice following ONC. **(A)** Scotopic b-wave amplitude recording of the ERG performed on the mice eyes ($n = 2-4$) dosed with different concentrations of ATN 224 (3.15, 6.25, 12.0, and 25 μM) after 7 days. **(B)** Significant difference in PERG amplitudes were observed in mouse eyes ($n = 6$) with crushed optic nerve in comparison with contralateral controls (** $P \leq 0.001$). There was significant restoration of PERG amplitudes observed in ONC + 2% SA-2 ($7.93 \pm 0.735 \mu\text{V}$, $n = 5$) eyes compared with ONC + PBS mice eyes ($5.04 \pm 0.714 \mu\text{V}$, $n = 5$), * $P < 0.05$, using 1-way Student-Newman-Keuls Method ANOVA when comparing ONC-ed groups. Values signify mean \pm SEM. The protective effect of 2% SA-2 was reversed by adding a known SOD inhibitor ATN-224 (3.15 $\mu\text{g}/\text{mL}$) observed as decrease in PERG amplitude in ONC

+ 2% SA-2 + ATN-224 mice eyes ($5.22 \pm 0.757 \mu\text{V}$, $n = 5$). (C) Sample PERG waveforms recorded from the ipsilateral and contralateral eyes to the pattern stimulus. (D) RBPMS-labeled RGCs were counted in mouse retinas ($n = 6$ per group). A significant ($*P < 0.05$) decline in RGC counts was observed 7 days following ONC in comparison with the contralateral controls. All pairwise multiple comparison procedures (Dunn's Method). There was a statistically significant protection of RGCs ($\#P = 0.032$) between ONC + 2% SA-2 ($n = 5$), treated cohort versus ONC + PBS ($n = 5$) treated group, t -test. (E) Representative fluorescent images of RBPMS-labeled RGCs in contralateral and ONC mouse retinas. Scale bar: 100 μm . (F) Immunohistochemical analysis for SOD1 from ONC + PBS ($n = 3$) or ONC + 2% SA-2 treated mice eyes ($n = 5$). SOD1 (in yellow) was localized to the cytoplasm of RGCs. The immunolabeling for SOD was evident in GCL, IPL, and OPL in control eyes and ONC + 2% SA-2 treated retinas. No staining for SOD1 was observed in ONC and PBS-treated group. β III tubulin immunolabeling (in green) was mainly localized to RGC somas and axons in GCL and NFL as well as their dendrites at IPL and with some staining at OPL layer. (G) Graph represents SOD1 immunofluorescence intensity calculated from the whole retinas of ONC + PBS-treated animals and ONC + 2% SA-2-treated mice. Data are represented as mean \pm SEM. (H, I) The number of β III Tubulin- and DAPI- positive cells in the GCL in tested retinal sections. Significances of intergroup differences were evaluated by t -test, although there was a trend in increase in number for both types of cells; however, no statistical significance was observed. n.s., not significant using t -test. (J) Immunohistochemical analysis for nitrotyrosine from control or ONC + PBS- or ONC + 2% SA-2-treated mice eyes. The nitrotyrosine (in red) signal was mainly localized to ONL, OPL, IPL, GCL, and NFL in the ONC + PBS or ONC + 2% SA-2 retinas. There were no visible differences in the nitrotyrosine levels in ONC + PBS and ONC + 2% SA-2 retinas. No significant nitrotyrosylation was observed in the control retinas with minimal staining present in the OPL and NFL of the retina.

(1204.45 ± 320.3 A.U.) in comparison with ONC + PBS-treated retinas (831.028 ± 216.526 A.U.). The number of β III Tubulin- (Fig. 6H) and DAPI- (Fig. 6I) positive cells in GCL per millimeter of the retina was also higher in 2% SA-2 treated groups by 21.0% and 20.2%, respectively.

As compound SA-2 is an NO-releasing prodrug, to rule out the possibility of unwanted protein nitrotyrosylation in retina after SA-2 administration, we performed the immunolabeling of retina with anti-nitrotyrosine antibody. We have not observed any significant increase in nitrotyrosine level in ONC-ed and SA-2 treated eyes as compared to ONC-ed and PBS eyes (Fig. 6J).

DISCUSSION

Previously, we reported an approach that combined “spontaneous” and pH-responsive NO donor³³ functional group with SOD mimetic (nitroxide) functional group (SA-2, Fig. 1) to both maintain a therapeutic level of NO and to scavenge superoxide,²¹ as a new approach for the treatment of glaucoma. Under conditions of H₂O₂-induced oxidative stress, the hybrid compound SA-2 protected the HUVECs with an EC₅₀ of 0.354 μM , scavenged the ROS, and maintained physiologically relevant level of eNOS.²⁸ We also demonstrated earlier that, compound SA-2 increased the SOD enzyme levels in 661W mouse photoreceptor neural cells²¹ and in primary human trabecular meshwork cells (Stankowska DL, Acharya S, unpublished observations, 2018).

Deficiency of the SOD enzyme leads to RGC and photoreceptor cell death as observed in ONC as well as in I/R-induced retinal injury animal models.^{15,34,35} Recently the direct effect of PEG-SOD in scavenging superoxide and preventing RGC loss following optic nerve transection was demonstrated.³² It was previously published that, 4-hydroxy-2,2,6,6-tetramethylpiperidinyl-1-oxyl, (4-hydroxy TEMPOL), a SOD mimetic compound, was able to prevent the production of hydroxyl radicals^{36,37} via oxidation of Fe²⁺ and protected neurons in in vitro and in vivo models of brain trauma, ischemic stroke, and Parkinson's disease.³⁸⁻⁴⁰ A SOD mimetic, 4-hydroxy TEMPOL used in a high concentration of 5 mM was found to significantly improve RGC survival in an in vitro model of TNF- α and hypoxia-induced RGC damage.⁴¹ In our current study, the compound SA-2, which is a structural analog of 4-hydroxy TEMPOL, was found to be very potent in protecting RGCs against hypoxic death in as low as 1 μM concentration in an adult retinal explant organotypic tissue culture system. Based on the ex vivo neuroprotective activity, we evaluated compound SA-2 in two rodent models of RGC death: an ONC and I/R-induced retinal injury. The ONC model recapitulates the pathological events including ROS production through glial activation, trophic factor deprivation, and

subsequent RGC death.⁴² Thaler et al.⁴³ demonstrated that intraperitoneal delivery of 20 mg/kg of 4-hydroxy TEMPOL protected rat retinas from ONC-induced damage. A hydrophobic analog of TEMPOL, TEMPOL-C8 acyl ester was more potent (1 mg/kg) when delivered intraperitoneally in protecting RGC from NMDA-induced excitotoxic death than its hydrophilic equivalent 4-hydroxy TEMPOL.⁴⁴

Here we have performed an ivt dosing of SA-2 to the retinas to demonstrate the potency and efficacy of SA-2 in protecting against RGC death in ONC and I/R injuries. The biodistribution results showed that 2% (75 mM) of single ivt dose of compound SA-2 (vitreous concentration \sim 15 mM) can provide 75-230 pM concentration of SA-2 to the retina and choroid in mouse eyes after 1 hour of dosing. As expected, this ivt dose of 2% of SA-2 prevented RGC death following ONC as well as I/R injury. Being a SOD mimetic, compound SA-2 was anticipated to increase the SOD levels in retina, an enzyme that is responsible for scavenging the superoxide as well as hydroxyl radicals. We have observed increased intensity of SOD1 in the ganglion cells and nerve fiber layers of the retinas following SA-2 treatment, which was diminished by adding a known SOD inhibitor ATN-224. We also observed that, there was no notable protein nitrotyrosylation in retinas from mice subjected to ONC and SA-2 injection, 7 days after the last dose of SA-2 administration.

Pressure-induced retinal ischemia (I/R) has been used as a model of retinal injury and has been described in many rodent species.^{45,46} The pathological features of this model are very similar to those seen in acute angle-closure glaucoma and central retinal artery occlusion.^{46,47} Here we have demonstrated that compound SA-2 provided neuroprotection to RGCs when administered prophylactically 48 hours before the I/R injury in mice. Our data clearly demonstrated that RGC function can be partially restored after prophylactic treatment of SA-2 in injured eyes. It is pertinent to mention that prophylactic treatment may not be the best option for a condition like ischemic ocular stroke, so further study is required to demonstrate the efficacy of treatment of SA-2 after I/R injury.

In summary, a small hybrid compound SA-2 with the potential of maintaining a physiological concentration of NO and effectively scavenging the ROS as shown by us in endothelial cells²⁸ was neuroprotective in the retina. Compound SA-2 was effective both therapeutically and prophylactically in three separate acute models of RGC death, including hypoxia, ONC, and I/R model and the neuroprotective activity is mediated by upregulation of SOD levels in the retinas following ONC. Compound SA-2 (2%) was found to be safe to the retina and bioavailable at the posterior segment via ivt injection. Compound SA-2 represents a next-generation drug that can provide neuroprotection in ocular neurodegenerative

diseases like glaucoma. Further study on sustained drug delivery of SA-2 is under progress.

Acknowledgments

The authors thank Raghu Krishnamoorthy, PhD, for several useful discussions and feedback on this project and Bindu Kodati, PhD, for help with the imaging.

Supported by Bright Focus Foundation grant (G2018056) to Suchismita Acharya (PI) and partial support from Fight for Sight Grant-In-Aid to Dorota L. Stankowska (PI).

Disclosure: **D.L. Stankowska**, None; **A. Dibas**, None; **L. Li**, None; **W. Zhang**, None; **V.R. Krishnamoorthy**, None; **S.H. Chavala**, None; **T.P. Nguyen**, None; **T. Yorio**, None; **D.Z. Ellis**, None; **S. Acharya**, None

References

- Quigley HA, Broman AT. The number of people with glaucoma worldwide in 2010 and 2020. *Br J Ophthalmol*. 2006;90:262-267.
- Lafuente MP, Villegas-Perez MP, Selles-Navarro I, Mayor-Torroglosa S, Miralles de Imperial J, Vidal-Sanz M. Retinal ganglion cell death after acute retinal ischemia is an ongoing process whose severity and duration depends on the duration of the insult. *Neuroscience*. 2002;109:157-168.
- Kaur C, Foulds WS, Ling E-A. Hypoxia-ischemia and retinal ganglion cell damage. *Clin Ophthalmol*. 2008;2:879-889.
- Yang M-H, Krishnamoorthy RR, Jong S-B, et al. Protein profiling of human nonpigmented ciliary epithelium cell secretome: the differentiation factors characterization for retinal ganglion cell line. *J Biomed Biotechnol*. 2011;2011:901329.
- Moreno MC, Campanelli J, Sande P, Sáenz DA, Keller Sarmiento MI, Rosenstein RE. Retinal oxidative stress induced by high intraocular pressure. *Free Radic Biol Med*. 2004;37:803-812.
- Munemasa Y, Ahn JH, Kwong JM, Caprioli J, Piri N. Redox proteins thioredoxin 1 and thioredoxin 2 support retinal ganglion cell survival in experimental glaucoma. *Gene Ther*. 2009;16:17-25.
- Kernt M, Arend N, Buerger A, et al. Idebenone prevents human optic nerve head astrocytes from oxidative stress, apoptosis, and senescence by stabilizing BAX/Bcl-2 ratio. *J Glaucoma*. 2013;22:404-412.
- Yokoyama Y, Maruyama K, Yamamoto K, et al. The role of calpain in an in vivo model of oxidative stress-induced retinal ganglion cell damage. *Biochem Biophys Res Commun*. 2014;451:510-515.
- Sucher NJ, Lipton SA, Dreyer EB. Molecular basis of glutamate toxicity in retinal ganglion cells. *Vision Res*. 1997;37:3483-3493.
- Ueda Y, Doi T, Nagatomo K, Nakajima A. In vivo activation of N-methyl-D-aspartate receptors generates free radicals and reduces antioxidant ability in the rat hippocampus: experimental protocol of in vivo ESR spectroscopy and microdialysis for redox status evaluation. *Brain Res*. 2007;1178:20-27.
- Bonfoco E, Krainc D, Ankarcona M, Nicotera P, Lipton SA. Apoptosis and necrosis: two distinct events induced, respectively, by mild and intense insults with N-methyl-D-aspartate or nitric oxide/superoxide in cortical cell cultures. *Proc Natl Acad Sci U S A*. 1995;92:7162.
- Kimura A, Namekata K, Guo X, Noro T, Harada C, Harada T. Targeting oxidative stress for treatment of glaucoma and optic neuritis. *Oxid Med Cell Longev*. 2017;2017:2817252.
- Tezel G. Oxidative stress in glaucomatous neurodegeneration: mechanisms and consequences. *Prog Retin Eye Res*. 2006;25:490-513.
- Warner HR. Superoxide dismutase, aging, and degenerative disease. *Free Radic Biol Med*. 1994;17:249-258.
- Yuki K, Ozawa Y, Yoshida T, et al. Retinal ganglion cell loss in superoxide dismutase 1 deficiency. *Invest Ophthalmol Vis Sci*. 2011;52:4143-4150.
- Arancio O, Lev-Ram V, Tsien RY, Kandel ER, Hawkins RD. Nitric oxide acts as a retrograde messenger during long-term potentiation in cultured hippocampal neurons. *J Physiol Paris*. 1996;90:321-322.
- Kornerup DD, Boding KL, Vladimir B, Elisabeth B. Cyclic guanosine monophosphate signalling pathway plays a role in neural cell adhesion molecule-mediated neurite outgrowth and survival. *J Neurosci Res*. 2007;85:703-711.
- Kohgami S, Ogata T, Morino T, Yamamoto H, Schubert P. Pharmacological shift of the ambiguous nitric oxide action from neurotoxicity to cyclic GMP-mediated protection. *Neurol Res*. 2010;32:938-944.
- Lei J, Vodovotz Y, Tzeng E, Billiar TR. Nitric oxide, a protective molecule in the cardiovascular system. *Nitric Oxide*. 2013;35:175-185.
- Maruhashi T, Noma K, Iwamoto Y, et al. Critical role of exogenous nitric oxide in ROCK activity in vascular smooth muscle cells. *PLoS One*. 2014;9:e109017.
- Acharya S, Rogers P, Krishnamoorthy RR, Stankowska DL, Dias HV, Yorio T. Design and synthesis of novel hybrid sydnonimine and prodrug useful for glaucomatous optic neuropathy. *Bioorg Med Chem Lett*. 2016;26:1490-1494.
- Tse DY, Kim SJ, Chung I, He F, Wensel TG, Wu SM. The ocular toxicity and pharmacokinetics of simvastatin following intravitreal injection in mice. *Int J Ophthalmol*. 2017;10:1361-1369.
- Stankowska DL, Mueller BH II, Oku H, Ikeda T, Dibas A. Neuroprotective effects of inhibitors of acid-sensing ion channels (ASICs) in optic nerve crush model in rodents. *Curr Eye Res*. 2018;43:84-95.
- Dibas A, Millar C, Al-Farfa A, Yorio T. Neuroprotective effects of psalmotoxin-1, an acid-sensing ion channel (ASIC) inhibitor, in ischemia reperfusion in mouse eyes. *Curr Eye Res*. 2018;43:921-933.
- Minton AZ, Phatak NR, Stankowska DL, et al. Endothelin B receptors contribute to retinal ganglion cell loss in a rat model of glaucoma. *PLoS One*. 2012;7:e43199.
- Porciatti V. Electrophysiological assessment of retinal ganglion cell function. *Exp Eye Res*. 2015;141:164-170.
- Fu X, Sun X, Zhang L, et al. Tuberos sclerosis complex-mediated mTORC1 overactivation promotes age-related hearing loss. *J Clin Invest*. 2018;128:4938-4955.
- Le DQ, Kuriakose AE, Nguyen DX, Nguyen KT, Acharya S. Hybrid nitric oxide donor and its carrier for the treatment of peripheral arterial diseases. *Sci Rep*. 2017;7:8692.
- Xia X, Wen R, Chou T-H, Li Y, Wang Z, Porciatti V. Protection of pattern electroretinogram and retinal ganglion cells by oncostatin M after optic nerve injury. *PLoS One*. 2014;9:e108524.
- Vine AK, Brewer GJ. Tetrathiomolybdate as an antiangiogenesis therapy for subfoveal choroidal neovascularization secondary to age-related macular degeneration. *Trans Am Ophthalmol Soc*. 2002;100:73-76; discussion 76-77.
- Juarez JC, Betancourt O Jr, Pirie-Shepherd SR, et al. Copper binding by tetrathiomolybdate attenuates angiogenesis and tumor cell proliferation through the inhibition of superoxide dismutase 1. *Clin Cancer Res*. 2006;12:4974-4982.
- Kanamori A, Catrinescu MM, Kanamori N, Mears KA, Beaubien R, Levin LA. Superoxide is an associated signal for apoptosis in axonal injury. *Brain*. 2010;133:2612-2625.
- Feelisch M, Ostrowski J, Noack E. On the mechanism of NO release from sydnonimines. *J Cardiovasc Pharmacol*. 1989;14(suppl 1):S13-S22.

34. Lindsey JD, Duong-Polk KX, Dai Y, Nguyen DH, Leung CK, Weinreb RN. Protection by an oral disubstituted hydroxylamine derivative against loss of retinal ganglion cell differentiation following optic nerve crush. *PLoS One*. 2013;8:e65966.
35. Nayak MS, Kita M, Marmor MF. Protection of rabbit retina from ischemic injury by superoxide dismutase and catalase. *Invest Ophthalmol Vis Sci*. 1993;34:2018-2022.
36. Mehta SH, Webb RC, Ergul A, Tawfik A, Dorrance AM. Neuroprotection by tempol in a model of iron-induced oxidative stress in acute ischemic stroke. *Am J Physiol Regul Integr Comp Physiol*. 2004;286:R283-R288.
37. Rak R, Chao DL, Pluta RM, Mitchell JB, Oldfield EH, Watson JC. Neuroprotection by the stable nitroxide Tempol during reperfusion in a rat model of transient focal ischemia. *J Neurosurg*. 2000;92:646-651.
38. Beit-Yannai E, Zhang R, Trembovler V, Samuni A, Shohami E. Cerebroprotective effect of stable nitroxide radicals in closed head injury in the rat. *Brain Res*. 1996;717:22-28.
39. Lipman T, Tabakman R, Lazarovici P. Neuroprotective effects of the stable nitroxide compound Tempol on 1-methyl-4-phenylpyridinium ion-induced neurotoxicity in the nerve growth factor-differentiated model of pheochromocytoma PC12 cells. *Eur J Pharmacol*. 2006;549:50-57.
40. Singh IN, Sullivan PG, Hall ED. Peroxynitrite-mediated oxidative damage to brain mitochondria: protective effects of peroxynitrite scavengers. *J Neurosci Res*. 2007;85:2216-2223.
41. Tezel G, Yang X. Caspase-independent component of retinal ganglion cell death, in vitro. *Invest Ophthalmol Vis Sci*. 2004;45:4049-4059.
42. Atlante A, Calissano P, Bobba A, Giannattasio S, Marra E, Passarella S. Glutamate neurotoxicity, oxidative stress and mitochondria. *FEBS Lett*. 2001;497:1-5.
43. Thaler S, Fiedorowicz M, Rejdak R, et al. Neuroprotective effects of tempol on retinal ganglion cells in a partial optic nerve crush rat model with and without iron load. *Exp Eye Res*. 2010;90:254-260.
44. Fiedorowicz M, Rejdak R, Schuettauf F, Wozniak M, Grieb P, Thaler S. Age-dependent neuroprotection of retinal ganglion cells by tempol-C8 acyl ester in a rat NMDA toxicity model. *Folia Neuropathol*. 2014;52:291-297.
45. Russo R, Cavaliere F, Berliocchi L, et al. Modulation of pro-survival and death-associated pathways under retinal ischemia/reperfusion: effects of NMDA receptor blockade. *J Neurochem*. 2008;107:1347-1357.
46. Osborne NN, Casson RJ, Wood JP, Chidlow G, Graham M, Melena J. Retinal ischemia: mechanisms of damage and potential therapeutic strategies. *Prog Retin Eye Res*. 2004;23:91-147.
47. Hughes WF. Quantitation of ischemic damage in the rat retina. *Exp Eye Res*. 1991;53:573-582.